Nanoscale Research Letters
a SpringerOpen Journal

NANO EXPRESS Open Access

Selective preparation of zero- and one-dimensional gold nanostructures in a TiO_2 nanocrystal-containing photoactive mesoporous template

Go Kawamura[1*], Teruhisa Okuno[2], Hiroyuki Muto[1,2] and Atsunori Matsuda[1,2]

Abstract

Nanocrystallized SiO_2-TiO_2 with tubular mesopores was prepared via the sol-gel technique. Gold was deposited in the tubular mesopores of the nanocrystallized SiO_2-TiO_2. The shape of the gold was varied from one-dimensional [1-D] to zero-dimensional [0-D] nanostructures by an increase in TiO_2 content and ultraviolet [UV] irradiation during gold deposition. 1-D gold nanostructures [GNSs] were mainly obtained in the mesopores when a small amount of TiO_2-containing mesoporous SiO_2-TiO_2 was used as a template, whereas the use of a template containing a large amount of TiO_2 led to the formation of shorter 1-D or 0-D GNSs. UV irradiation also resulted in the formation of 0-D GNSs.

PACS: 06.60.Jn (sample preparation); 81.07.Gf (nanowires); 81.16.Be (chemical synthesis methods).

Keywords: mesoporous, titania, template, gold, nanostructures, shape control, photocatalysis, surface plasmon resonance

Introduction

Gold nanostructures [GNSs] have been attracting much attention because of the high chemical stability coincident with their unique optoelectronic properties, which are dependent on the morphology of the GNSs [1-4]. Surface plasmon resonance [SPR] is one of the most interesting properties of one-dimensional [1-D] GNSs [2-5]. The wavelength of SPR is affected by the length, diameter, and aspect ratio of the 1-D GNSs [6,7]. Aligned GNSs perform polarization of light [8-10]. Such multifunctionality of the 1-D GNSs opens up new application fields such as wavelength-sensitive nonlinear optical devices and polarization filters [8,9,11]. Several methods for synthesizing GNSs including 1-D GNSs have been reported. These methods include photochemical and electrochemical deposition [12,13] and seeding growth methods [14,15]. In these methods, however, the GNSs are suspended in a solvent. Therefore, the GNSs are required to be immobilized in a designed fashion in/on a solid matrix for various kinds of practical applications. The immobilization process for GNSs still requires further development [3,10,16].

On the other hand, the use of hard templates such as anodic alumina and mesoporous silica for the synthesis of 1-D GNSs makes the complicated immobilization processes redundant, and several related studies have been reported [17,18]. Those methods using hard templates are also advantageous to control the diameter and dispersion state of 1-D GNSs because they depend on the pore structure. However, methods that control the morphology of the 1-D GNSs have several problems. For example, the elongation of the 1-D GNSs requires more gold to be deposited in the template. This obstructs, for example, the investigation of the shape-dependent properties of the GNSs. Therefore, a novel method to control the morphology of the 1-D GNSs in hard templates without changing the gold amount is eagerly demanded.

In this work, nanocrystallized SiO_2-TiO_2 with tubular mesopores was prepared and used as an active template.

* Correspondence: gokawamura@ee.tut.ac.jp
[1]Department of Electrical and Electronic Information Engineering, Toyohashi University of Technology, 1-1 Hibarigaoka, Tempaku-cho, Toyohashi, Aichi, 441-8580, Japan
Full list of author information is available at the end of the article

0-D and 1-D GNSs were deposited in the tubular mesopores. The shape of the GNSs was observed, and the SPR characteristics were measured. It is known that TiO_2 nanocrystals generate electrons through heating and ultraviolet [UV] irradiation. In this study, the generated electrons were found to transfer to the Au^{3+} ions. As such, the deposition rate of the GNSs can be controlled by controlling the amount of electrons generated. As a result, 0-D and 1-D GNSs are selectively deposited.

Experimental methods

Materials

Pluronic P123 ($(EO)_{20}(PO)_{70}(EO)_{20}$, poly(ethylene oxide), and poly(propylene oxide)) was purchased from Sigma-Aldrich (St. Louis, MO, USA). Tetraethoxysilane [TEOS] and 3-aminopropyltriethoxysilane [APTES] were obtained from Shin-Etsu Chemical Co., Ltd. (Tokyo, Japan). Titanium tetra-*n*-butoxide [TTB] and $HAuCl_4$ were acquired from Wako Pure Chemical Industries, Ltd. (Osaka, Japan) and Kishida (Osaka, Japan), respectively.

Synthesis of mesoporous template

The preparation procedure of 20Ti is described as a typical example. A mixture of P123 (1.74 g), NaCl (2.92 g), and 1 mM HCl (100 mM) was added to TEOS (4.18 g) and stirred at 35°C for 24 h. TTB (1.70 g) was then added to the solution and stirred further for 6 h. For the preparation of $(100\text{-}x)SiO_2{\cdot}xTiO_2$, only the ratio of TEOS to TTB was varied. The stirred solution was transferred into an autoclave vessel and kept at 100°C for 4 h. The precipitated powder was collected by suction filtration, then washed with ion-exchanged water [IEW] and ethanol, and dried in an ambient environment. The obtained powder was calcined at 550°C for 5 h to remove the surfactant from the mesopore.

Loading of Au

The obtained powder was immersed in the 1 wt.% APTES solution (in ethanol) and stirred at 25°C for 3 h. The powder was then filtered with suction, washed with ethanol, and dried at 60°C in air. The amino-functionalized powder was mixed into a 1-mM $HAuCl_4$ aqueous solution and stirred at 25°C for 2 h. After the suction filtration, the product was washed with IEW and dried in an ambient environment. The product was then calcined at 350°C for 3 h (at a heating rate of 1°C/min) with or without UV irradiation (USHIO SP-9, 230-440 nm, 2.5 mW/cm^2 at 365 nm).

Characterization

X-ray diffraction [XRD] measurements were performed using a Rigaku RINT 2000 diffractometer (Rigaku Corporation, Tokyo, Japan) with CuKα radiation (λ = 1.5406 Å). Transmission electron microscopy [TEM] images and energy dispersive spectroscopy [EDS] were taken using a Hitachi H-800 transmission electron microscope (High-Technologies Corporation, Chiyoda, Tokyo, Japan) and a JEOL JEM-2100F (JEOL, Ltd., Akishima, Tokyo, Japan) transmission electron microscope operating at 200 kV. UV/visible-near infrared diffuse reflectance [Vis-NIR DR] spectra were measured using a JASCO V-670 UV-Vis-NIR spectroscope (JASCO Corporation, Tokyo, Japan).

Results and discussion

In the XRD pattern of the mesoporous $100SiO_2$ template [0Ti], amorphous SiO_2 was observed as a halo at ca. 23°. On the other hand, the $80SiO_2{\cdot}20TiO_2$ template [20Ti] showed several peaks consistent with both anatase and rutile TiO_2, as well as amorphous SiO_2 (Figure 1A). The peaks of the TiO_2 crystals appeared stronger in the pattern of the $50SiO_2{\cdot}50TiO_2$ template [50Ti] in comparison with those of 20Ti. A TEM observation of these templates revealed that all of them possessed a 2-D hexagonal mesoporous structure with the same caliber of ca. 7 nm (Figures 1B, C, D). The high-resolution TEM images of 20Ti and 50Ti showed ca. 4-nm crystals with a fringe spacing of 3.52 Å, which were well dispersed in the samples (insets of Figures 1C, D). The fringe spacing is consistent with the *d* value of {011} planes of anatase TiO_2. This proves that the templates consist of pure amorphous SiO_2, or SiO_2 and well-dispersed TiO_2 nanocrystals, forming a 2-D hexagonal mesoporous structure.

Particles without mesopores were rarely observed in the TEM images of 20Ti and 50Ti prepared by aging in water at 100°C for 4 h. On the other hand, 20Ti (and 50Ti) aged for 24 h in water at 100°C showed the formation of large nonporous particles outside the mesoporous structure (Figure 2A). The components of the nonporous particles and mesoporous region were solely attributed to TiO_2 and SiO_2, respectively (Figure 2B). Thus, the TiO_2 crystal formation in our samples should be based on the dissolution and deposition of the TiO_2 component by aging in hot water, where the TiO_2 component in the SiO_2-TiO_2 gel system is dissolved into water and then reprecipitated as crystalline TiO_2 [19,20]. The short aging time in hot water resulted in the suppression of large TiO_2 particle formation and the sufficient deposition of TiO_2 nanocrystals with a highly dispersed state on/in the mesoporous matrix. In this work, therefore, the aging time of 4 h was employed to prepare the templates, which possess almost the same pore size and structure regardless of the TiO_2 content. The molar ratio of SiO_2 to TiO_2 in the mesoporous region was checked by EDS, and it was found to be comparable to the nominal molar ratio. By using the templates, the effect of the TiO_2 nanocrystals on the shape of the 1-D GNSs can be investigated due to the sufficient formation of interfaces between the deposited Au and TiO_2 nanocrystals.

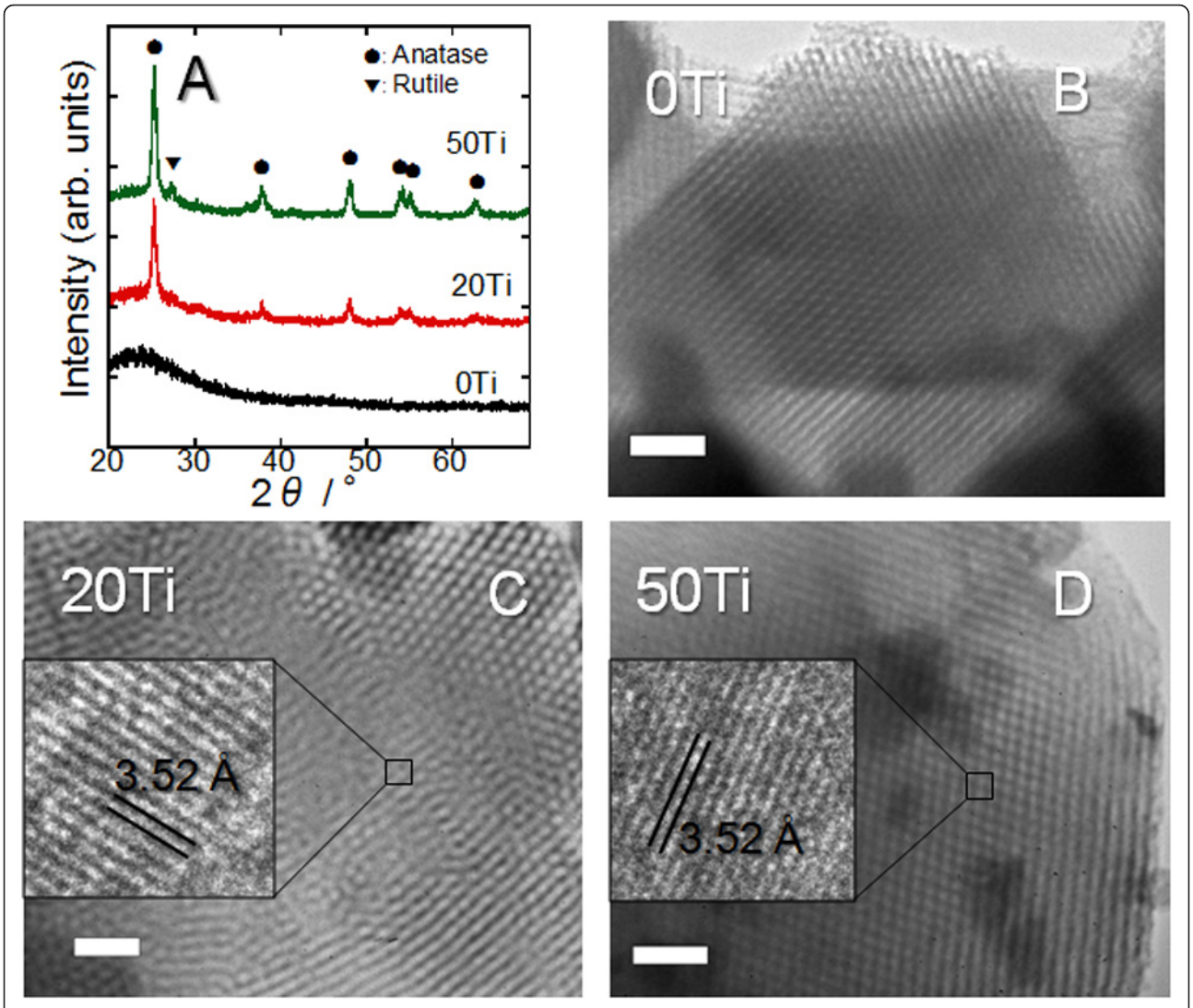

Figure 1 XRD patterns and TEM images of 0Ti, 20Ti, and 50Ti. (**A**) XRD patterns of 0Ti, 20Ti, and 50Ti. (**B**-**D**) The corresponding TEM images of the 0Ti, 20Ti, and 50Ti (scale bars, 50 nm). The insets in C and D are HR TEM images of the squared regions.

Long 1-D GNSs were formed in 0Ti after Au loading (Figure 3A). At the beginning of the Au loading, the Au^{3+} ions adsorb to the amino groups on the wall of the mesopores. Heat treatment of the resultant powder causes decomposition of the amino group-containing organic matter. The Au^{3+} ions are released and partly reduced to Au^{+} ions and Au atoms by electrons provided from the decomposed organic matter. The Au atoms agglomerate and form Au nanoclusters, and then the Au ions released from the amino groups are reduced on the Au nanoclusters by autocatalysis of Au [21,22], causing the Au metal to grow. Since the growth of Au occurs in the tubular mesopores, the final shape of the Au should be 1-D or 0-D GNSs. A morphology change of the GNSs was then investigated when the content of TiO_2 in the template was varied. The length of the 1-D GNSs formed in 20Ti (Figure 3B) was shorter than that deposited in 0Ti, whereas 0-D GNSs were predominantly obtained in 50Ti (Figure 3C). These results indicate that an increase in TiO_2 content leads to a shortening of the 1-D GNSs. This is presumably because thermoexcited conduction electrons are generated from TiO_2, and these generated electrons transfer to the Au ions to accelerate their reduction [23]. TiO_2 heated at 350°C generates approximately 8.8×10^{13} times as many thermoexcited electrons as TiO_2 does at room temperature [24]. Therefore, the amount of electrons supplied to the Au ions increases as the TiO_2 content increases. As a result, Au metal is rapidly deposited prior to its migration for the formation of long 1-D GNSs. Therefore, 0-D GNSs were predominantly formed in the tubular mesopores by using templates containing more than 50 mol% TiO_2.

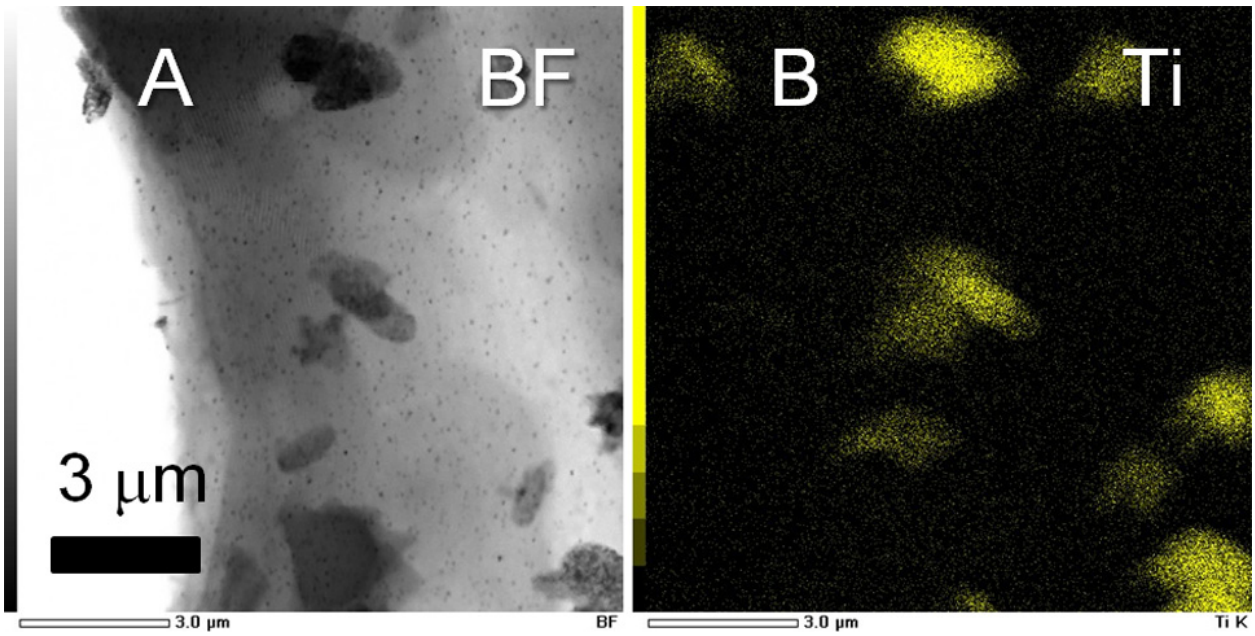

Figure 2 TEM image and Ti elemental mapping of 20 Ti. (**A**) Bright field TEM image and (**B**) Ti elemental mapping of 20Ti treated in water at 100°C for 24 h.

1-D GNSs deposited in 0Ti showed two extinction peaks in the diffuse reflectance [DR] spectrum: a sharp extinction peak at 500 nm and a broad extinction peak spreading over the whole region of the NIR region (Figure 3D). The shorter- and longer-wavelength extinctions are attributed to the transverse mode of SPR and the light scattering by fairly long 1-D GNSs [25], respectively. The length of the 1-D GNSs was shortened when 20Ti was used. An extinction peak appeared at around 600 nm, and the extinction intensity at wavelengths longer than 1,200 nm increased. This is presumably due to the shortening of the 1-D GNSs, which leads to a decrease in the light scattering intensity of the long 1-D GNSs (appearing over the whole NIR region) and an increase in the longitudinal SPR [LSPR] mode caused by the short 1-D GNSs (appearing at the NIR region toward the shorter wavelength side, e.g. 600 nm and approximately 2,000 nm in this case). With 30Ti, the LSPR peaks blue-shifted and appeared at 580 and approximately 900 nm. When 50Ti was used, only 0-D GNSs were deposited accompanied by a 520-nm peak, which is attributed to the SPR of the 0-D GNSs. By the use of a mesoporous SiO_2 template containing less than 30 mol% TiO_2, 1-D GNSs exhibiting LSPR, which is excited by NIR light, are deposited regardless of the presence of TiO_2 nanocrystallites in the template.

Since TiO_2 is known as a photocatalyst that generates electrons and holes by UV irradiation, the effects of UV irradiation during Au loading on the shape of the GNSs were investigated. As for the TiO_2 crystalline phases, anatase TiO_2 was widely recognized as the most suitable phase for photocatalysis [26,27]; but recent reports suggest that mixed rather than single phases can be even more active [28,29]. Also, since the TiO_2 nanocrystals in our samples possess diameters of a few nanometers, which are almost the optimum size for photocatalysis [26], UV irradiation of the templates should generate charges and influence the shape of the GNSs. In the case where 0Ti was used, 1-D GNSs with a length of 10 to 100 nm were deposited regardless of the UV irradiation (Figures 4A, B). It is worth mentioning that the 1-D GNSs in 0Ti were fabricated with a short length by shortening the calcination time in order to discuss the shift of the resonant wavelength in the measurable NIR region. In the DR spectra, the LSPR wavelengths of the samples prepared with and without UV irradiation were 930 and 990 nm, respectively. The wavelengths were slightly shifted, and the LSPR extinction intensity decreased slightly upon UV irradiation (Figure 4C). The results reveal that UV irradiation has only a minor effect on the shape of the deposited 1-D GNSs when 0Ti is used. On the other hand, although 1-D GNSs with a length of 10 to 400 nm were obtained in 20Ti without UV irradiation (Figure 4D), 0-D GNSs were predominantly deposited when UV irradiation was carried out (Figure 4E). The extinction peaks in the NIR region almost disappeared when the sample was exposed to UV irradiation (Figure 4F). These results clearly show that UV irradiation during Au loading in 20Ti influences the shape of the GNSs. Furthermore, since the

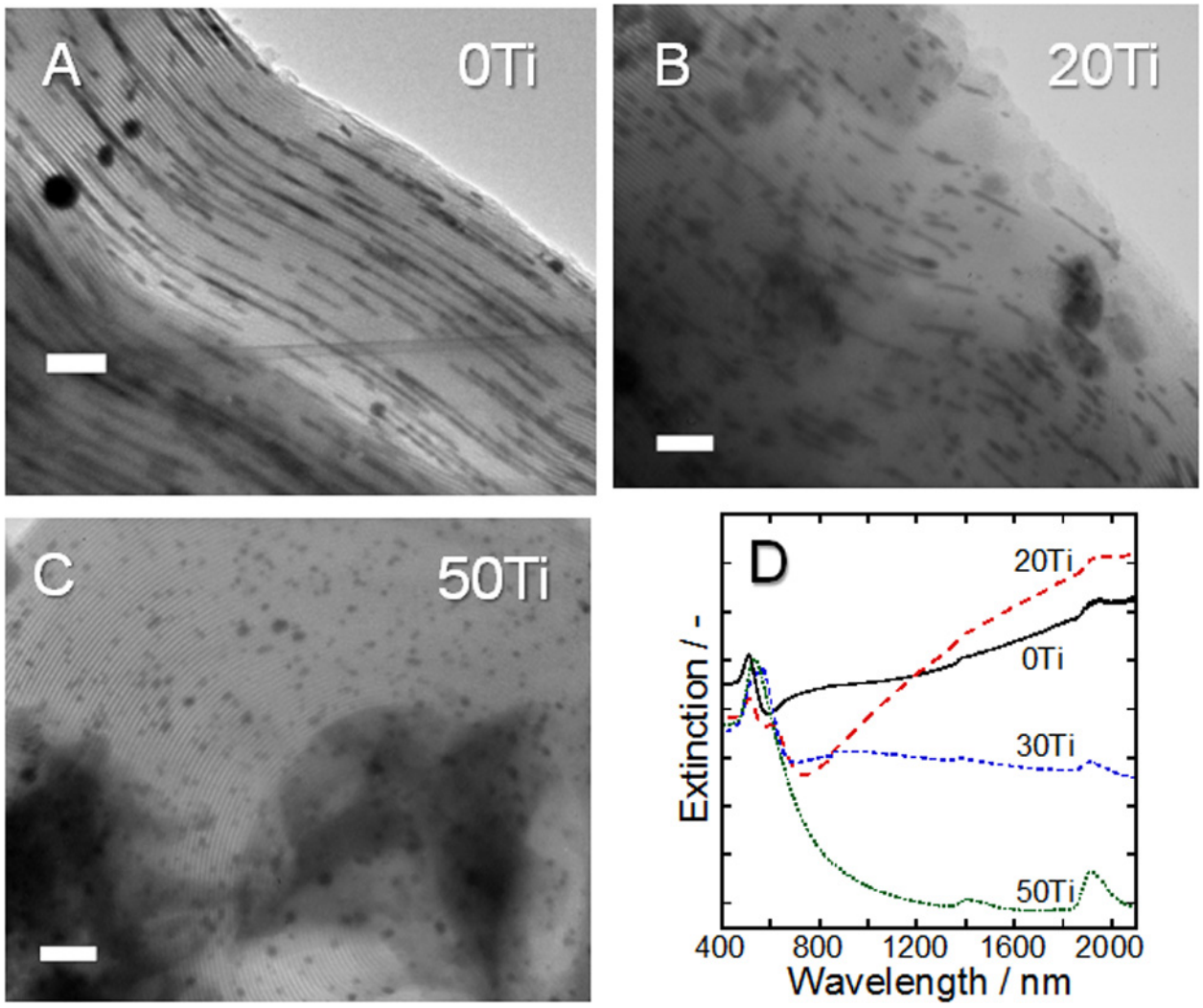

Figure 3 TEM images and DR spectra after Au deposition. TEM images of (**A**) 0Ti, (**B**) 20Ti, and (**C**) 50Ti after Au deposition (scale bars, 100 nm). (**D**) The corresponding DR spectra.

GNSs are insensitive toward UV light, it is evident that the photocatalytic activity of TiO_2 affects the shape of the GNSs in the template.

Two mechanisms were considered for the preferential formation of 0-D GNSs by UV irradiation: acceleration of the Au-ion reduction rate by the generated electrons or oxidation of deposited Au metal by the generated holes. In the case where UV irradiation at room temperature was carried out on the Au ion-adsorbed 20Ti, an increase in extinction intensity was observed from the Vis to the NIR region (Figure 5A). The increased extinction was attributed to the formation of 1-D GNSs of various lengths because of the wide wavelength region of SPR. On the other hand, UV irradiation of 0Ti resulted in a slight increase in extinction intensity over a similarly wide wavelength region (Figure 5A). This is probably due to the marginal deposition of GNSs by UV irradiation, which partly decomposes the organic matter adsorbed on the mesoporous wall, and thus, a small number of electrons are generated that reduce Au ions. This would explain the spectral change in Figure 4C, where the thermal and photo decomposition of the organic matter occurs simultaneously at the beginning of the Au loading process; thus, the Au reduction rate is slightly increased. Furthermore, since the variation of the extinction intensity in 20Ti is much larger than that in 0Ti, it is clear that UV irradiation accelerates the reduction of Au ions as a result of the electrons generated from TiO_2. On the other hand, UV irradiation after the thermal deposition of 1-D GNSs in 20Ti led to little change in the DR spectra (Figure 5B). This indicates that the holes, which are expected to oxidize the deposited 1-D GNSs to Au ions,

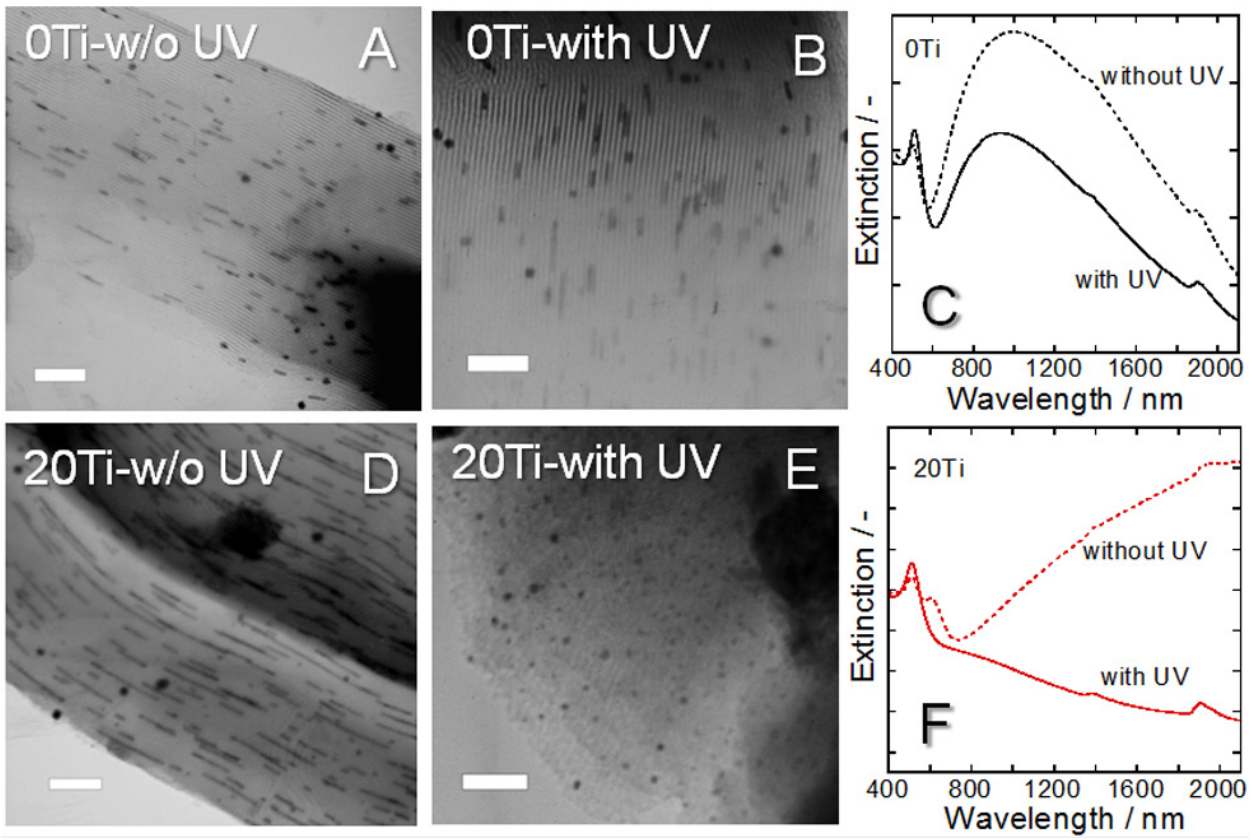

Figure 4 TEM images of 0Ti and 20Ti with their corresponding DR spectra after Au deposition. TEM images of 0Ti after thermal Au deposition were carried out (**A**) Without or (**B**) with simultaneous UV irradiation. (**C**) The corresponding DR spectra of A and B. TEM images of 20Ti after thermal Au deposition was carried out (**D**) without or (**E**) with simultaneous UV irradiation. (**F**) The corresponding DR spectra of D and E. (scale bars, 100 nm).

have negligible effect on the shape change in the GNSs. Thus, it is concluded that the photocatalysis of TiO_2 causes the reduction of the gold ions rather than oxidation of the Au metal. The generated holes may be consumed to decompose organic matter adsorbed on the wall of the template. In addition, UV irradiation of the 1-D GNSs deposited in 0Ti also resulted in no change in the DR spectra.

The results obtained suggest the probable mechanism of Au deposition by the simultaneous heat treatment and UV irradiation, where the predominant formation of 0-D GNSs was observed (Figure 4E). The heat treatment causes the decomposition of organic matter adsorbed on the wall of the template. This results in the partial reduction of Au^{3+} ions, followed by the formation of scattered Au nanoclusters. The partially reduced Au ions are released from their electrostatic adsorption to the amino groups and associated with the oxygen atoms on the wall surface of the matrix, enabling mobility of the Au ions [30]. The Au ions, therefore, can reach the neighboring Au nanoclusters and are reduced on the surface of the nanoclusters by autocatalysis of Au [21,22], resulting in the formation of 1-D GNSs because the growth of Au occurs in the tubular mesopores. Thermally excited electrons of TiO_2 accelerate the reduction rate of the Au ions; thus, a large content of TiO_2 in the template leads to the preferential formation of 0-D GNSs. Furthermore, UV irradiation also accelerates the reduction rate of the Au ions. Therefore, the combination of heat treatment and UV irradiation leads to a fast rate of Au deposition. The time taken for the movement of the Au ions is shortened, and the formation of 0-D GNSs instead of 1-D GNSs becomes dominant. By optimizing the heating and UV irradiation condition of our method, 1-D and 0-D GNSs are selectively deposited regardless of the composition of the template, where the amount of deposited Au atoms is constant but the shape of the GNSs is different.

Conclusion

We have demonstrated the preparation of TiO_2 nanocrystal-containing mesoporous templates and deposited 1-D or 0-D GNSs in the as-formed tubular mesopores.

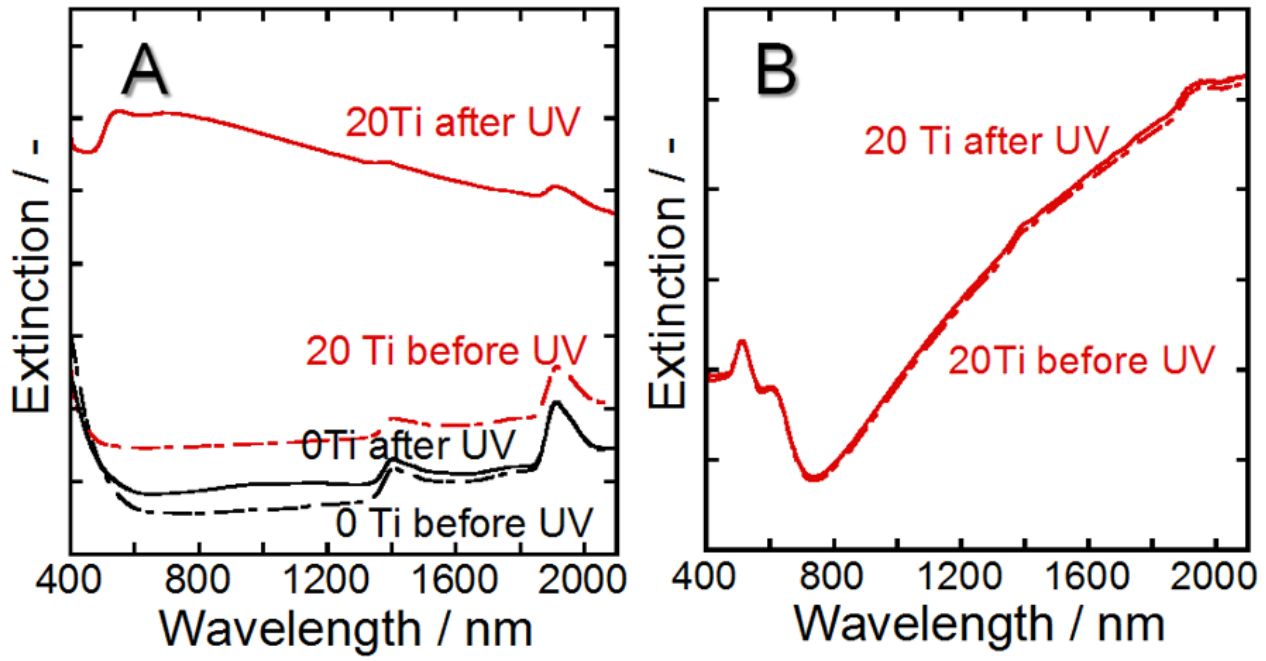

Figure 5 DR spectra of Au^{3+} ion-adsorbed 20Ti and 0Ti and of 1-D GNSs. (**A**) DR spectra of Au^{3+} ion-adsorbed 20Ti and 0Ti before and after UV irradiation (no heat treatment). (**B**) DR spectra of the 1-D GNSs thermally pre-deposited in 20Ti before and after UV irradiation.

Since the provision of thermally generated electrons from TiO_2 increased when a template contained a large amount of TiO_2, Au ions were rapidly reduced and deposited as shorter 1-D or 0-D GNSs. Similarly, UV irradiation during Au deposition in the TiO_2-containing template produced electrons photocatalytically and accelerated the Au deposition rate, leading to the dominant formation of 0-D GNSs.

Abbreviations

APTES: 3-aminopropyltriethoxysilane; DR: diffuse reflectance; EDS: energy dispersive spectroscopy; GNSs: gold nanostructures; HR: high-resolution; IEW: ion-exchanged water; LSPR: longitudinal surface plasmon resonance; NIR: near infrared; 1-D: one-dimensional; SPR: surface plasmon resonance; TEOS: tetraethoxysilane; TEM: transmission electron microscopy; TTB: titanium tetra-*n*-butoxide; UV: ultraviolet; Vis: visible; XRD: X-ray diffraction.

Acknowledgements

This work was supported by Grants-in-Aid for Young Scientists (Start-up) 21860045 and Young Scientists (B) 22760539 from the Japan Society for the Promotion of Science (JSPS).

Author details

[1]Department of Electrical and Electronic Information Engineering, Toyohashi University of Technology, 1-1 Hibarigaoka, Tempaku-cho, Toyohashi, Aichi, 441-8580, Japan [2]Department of Environmental and Life Sciences, Toyohashi University of Technology, 1-1 Hibarigaoka, Tempaku-cho, Toyohashi, Aichi, 441-8580, Japan

Authors' contributions

GK, TO, and AM designed the study. TO performed the experiments with help from GK and AM. GK and AM contributed in drafting the manuscript. All authors edited and approved the manuscript.

Competing interests

The authors declare that they have no competing interests.

Received: 6 September 2011 Accepted: 5 January 2012
Published: 5 January 2012

References

1. Daniel MC, Astruc D: **Gold nanoparticles: assembly, supramolecular chemistry, quantum-size-related properties, and applications toward biology, catalysis, and nanotechnology.** *Chem Rev* 2004, **104**:293.
2. Perez-Juste J, Pastoriza-Santos I, Liz-Marzan LM, Mulvaney P: **Gold nanorods: synthesis, characterization and applications.** *Coord Chem Rev* 2005, **249**:1870.
3. Kawamura G, Yong Y, Nogami M: **Facile assembling of gold nanorods with large aspect ratio and their surface-enhanced Raman scattering properties.** *Appl Phys Lett* 2007, **90**:261908.
4. Kawamura G, Yong Y, Nogami M: **End-to-end assembly of CTAB-stabilized gold nanorods by citrate anions.** *J Phys Chem C* 2008, **112**:10632.
5. Mulvaney P, Perez-Juste J, Giersig M, Liz-Marzan LM, Pecharroman C: **Drastic surface plasmon mode shifts in gold nanorods due to electron charging.** *Plasmonics* 2006, **1**:61.
6. Brioude A, Jiang XC, Pileni MP: **Optical properties of gold nanorods: DDA simulations supported by experiments.** *J Phys Chem B* 2005, **109**:13138.
7. Huang X, Neretina S, El-Sayed MA: **Gold nanorods: from synthesis and properties to biological and biomedical applications.** *Adv Mater* 2009, **21**:4880.
8. Wilson O, Wilson GJ, Mulvaney P: **Laser writing in polarized silver nanorod films.** *Adv Mater* 2002, **14**:1000.
9. Perez-Juste J, Rodriguez-Gonzalez B, Mulvaney P, Liz-Marzan LM: **Optical control and patterning of gold nanorod-poly(vinyl alcohol) nanocomposite films.** *Adv Funct Mater* 2005, **15**:1065.
10. Murphy CJ, Orendorff CJ: **Alignment of gold nanorods in polymer composites and on polymer surfaces.** *Adv Mater* 2005, **17**:2173.
11. Tsutsui Y, Hayakawa T, Kawamura G, Nogami M: **Tuned longitudinal surface plasmon resonance and third-order nonlinear optical properties of gold nanorods.** *Nanotechnology* 2011, **22**:275203.

12. Esumi K, Matsuhisa K, Torigoe K: **Preparation of rodlike gold particles by UV irradiation using cationic micelles as a template.** *Langmuir* 1995, **11**:3285.
13. Yu YY, Chang SS, Lee CL, Wang CRC: **Gold nanorods: electrochemical synthesis and optical properties.** *J Phys Chem B* 1997, **101**:6661.
14. Jana NR, Gearheart L, Murphy CJ: **Seed-mediated growth approach for shape-controlled synthesis of spheroidal and rod-like gold nanoparticles using a surfactant template.** *Adv Mater* 2001, **13**:1389.
15. Kawamura G, Nogami M: **Application of a conproportionation reaction to a synthesis of shape-controlled gold nanoparticles.** *J Cryst Growth* 2009, **311**:4462.
16. Gole A, Orendorff CJ, Murphy CJ: **Immobilization of gold nanorods onto acid-terminated self-assembled monolayers via electrostatic interactions.** *Langmuir* 2004, **20**:7117.
17. Sawitowski T, Miquel Y, Heilmann A, Schmid G: **Optical properties of quasi one-dimensional chains of gold nanoparticles.** *Adv Funct Mater* 2001, **11**:435.
18. Li Z, Kubel C, Parvulescu VI, Richards R: **Size tunable gold nanorods evenly distributed in the channels of mesoporous silica.** *ACS Nano* 2008, **2**:1205.
19. Matsuda A, Kotani Y, Kogure K, Tatsumisago M, Minami T: **Transparent anatase nanocomposite films by the sol-gel process at low temperatures.** *J Am Ceram Soc* 2000, **83**:229.
20. Kotani Y, Matsuda A, Tatsumisago M, Minami T, Umezawa T, Kogure T: **Formation of anatase nanocrystals in sol-gel derived TiO_2-SiO_2 thin films with hot water treatment.** *J Sol-Gel Sci Tech* 2000, **19**:585.
21. Rodriguez-Sanchez L, Blanco MC, Lopez-Quintela MA: **Electrochemical synthesis of silver nanoparticles.** *J Phys Chem B* 2000, **104**:9683.
22. Jana NR, Gearheart L, Murphy CJ: **Evidence for seed-mediated nucleation in the chemical reduction of gold salts to gold nanoparticles.** *Chem Mater* 2001, **13**:2313.
23. Mizuguchi J: **Titanium dioxide as a combustion-assisting agent.** *J Electrochem Soc* 2001, **148**:J55.
24. Mizuguchi J, Shinbara T: **Disposal of used optical disks utilizing thermally-excited holes in titanium dioxide at high temperatures: a complete decomposition of polycarbonate.** *J Appl Phys* 2004, **96**:3514.
25. Liz-Marzan LM: **Tailoring surface plasmon resonance through the morphology and assembly of metal nanoparticles.** *Langmuir* 2006, **22**:32.
26. Carreon MA, Choi SY, Mamak M, Choprab N, Ozin GA: **Pore architecture affects photocatalytic activity of periodic mesoporous nanocrystalline anatase thin films.** *J Mater Chem* 2007, **17**:82.
27. Aprile C, Corma A, Garcia H: **Enhancement of the photocatalytic activity of TiO_2 through spatial structuring and particle size control: from subnanometric to submillimetric length scale.** *Phys Chem Chem Phys* 2008, **10**:769.
28. Wu JM, Qi B: **Low-temperature growth of a nitrogen-doped titania nanoflower film and its ability to assist photodegradation of rhodamine B in water.** *J Phys Chem C* 2007, **111**:666.
29. We JM, Antonietti A, Gross S, Bauer M, Smarsly BM: **Ordered mesoporous thin films of rutile TiO_2 nanocrystals mixed with amorphous Ta_2O_5.** *Chem Phys Chem* 2008, **9**:748.
30. Matsubara K, Tatsuma T: **Morphological changes and multicolor photochromism of Ag nanoparticles deposited on single-crystalline TiO_2 surfaces.** *Adv Mater* 2007, **19**:2802.

doi:10.1186/1556-276X-7-27
Cite this article as: Kawamura *et al.*: Selective preparation of zero- and one-dimensional gold nanostructures in a TiO_2 nanocrystal-containing photoactive mesoporous template. *Nanoscale Research Letters* 2012 **7**:27.